



Surface and thermal behavior of chitosan/poly(ethylene oxide) blends

Jolanta Kowalonek

To cite this article: Jolanta Kowalonek (2016) Surface and thermal behavior of chitosan/poly(ethylene oxide) blends, *Molecular Crystals and Liquid Crystals*, 640:1, 78-89, DOI: [10.1080/15421406.2016.1255518](https://doi.org/10.1080/15421406.2016.1255518)

To link to this article: <http://dx.doi.org/10.1080/15421406.2016.1255518>



Published online: 14 Dec 2016.



Submit your article to this journal [↗](#)



Article views: 2



View related articles [↗](#)



View Crossmark data [↗](#)

Surface and thermal behavior of chitosan/poly(ethylene oxide) blends

Jolanta Kowalonek

Nicolaus Copernicus University in Toruń, Faculty of Chemistry, Toruń, Poland

ABSTRACT

Chitosan/poly(ethylene oxide) (PEO) blends of different component ratios, in the form of films, have been prepared. Structure, hydrophilicity, morphology and thermal behavior of the samples have been examined by Fourier transform infrared spectroscopy (ATR-FTIR), contact angle measurements, atomic force microscopy (AFM) and differential scanning calorimetry (DSC).

The studies revealed weak interactions between chitosan and PEO suggesting immiscibility of the components in the blends. However, stronger interactions owing to hydrogen bonding between blend components were found for chitosan/PEO (80/20) blend.

Morphology of the blend surfaces was affected by the crystallinity of PEO and was dependent on the sample composition.

KEYWORD


chitosan; poly(ethylene oxide); polymer blends; surface studies; DSC

Introduction

Chitosan is a linear polysaccharide composed of $\beta(1\rightarrow4)$ -2-amino-2-deoxy-D-glucopyranose (D-glucosamine) and $\beta(1\rightarrow4)$ -2-acetamido-2-deoxy-D-glucopyranose (*N*-acetyl-D-glucosamine), which means that it is a copolymer. Chitosan is acquired from chitin by treating it with aggressive deacetylation solution, for instance 50% solution of sodium hydroxide at raised temperature. In this process, part or all acetyl groups from acetamido groups of chitin is removed and amino groups are formed. Chitin is acquired from crustacean shells, which means that chitin and chitosan are the examples of renewable resources [1].

Chitosan became a versatile polymer owing to its unique properties. Features such as non-toxicity [2], biocompatibility [3, 4], biodegradability [5], antibacterial activity [6,7] made this polymer useful in medicine in wound dressing or drug carriers [8–10], pharmaceutical industry in weight loss products [11], cosmetic industry in creams [12], food industry, environmental field for removing metals or dyes from wastewater [13, 14], agriculture for controlled agrochemical release or seed coatings [15–16].

Poly(ethylene oxide), PEO, is a linear polyether having the structure $(-\text{CH}_2-\text{CH}_2-\text{O})_n$. It is a semicrystalline polymer with the melting temperature of the crystalline phase equal to 65°C and the glass transition temperature of the amorphous phase equal to -60°C. The degree of the crystallinity is about 70–85%. PEO forms lamellae which are arranged in spherulites. In the crystalline state, it adopts a helical configuration in which 7 monomer units and two turns exist per identity period equal to 1.93 nm (7/2 helix). Groups: $-\text{O}-\text{CH}_2-$, CH_2-CH_2- , $-\text{CH}_2-\text{O}-$

CONTACT Jolanta Kowalonek  jolak@umk.pl

Color versions of one or more of the figures in the article can be found online at www.tandfonline.com/gmcl.

© 2016 Taylor & Francis Group, LLC

form conformation: trans, gauche, trans, respectively. In a molten state, the PEO conformation becomes less ordered and trans conformation is predominant [17–19].

PEO is widely used in industry due to its non-toxicity, compatibility and good water solubility. It is deployed in pharmacy to produce ointments, suppositories, tablet coatings. In cosmetic industry, PEO is an ingredient of creams, lotions or powders. It is used in manufacture of disposable packaging, especially films for agriculture [17–19].

Both polymers can be mixed to acquire new materials with altered properties with respect to the features of the individual components. Chitosan was used for formation of nanofibers by electrospinning technique, but for pure chitosan the process appeared to be complicated, therefore it was often blended with synthetic polymer such as PEO. Various useful applications of this system have been tested. The chitosan/PEO nonwoven fibers were prepared for air and water filtration systems [20]. The chitosan/PEO nanofibers were treated with air dielectric barrier discharge plasma to activate the surface and immobilize the enzyme for biological applications [21]. The electrospun chitosan/PEO nanofibers were studied in terms of antimicrobial activity [22, 23], morphology and thermal properties [24–26]. Surface properties of chitosan/PEO nanofibers with the addition of gelatin and/or crosslinked were analyzed with XPS, SEM, XRD and Zeta-potential measurements [27].

Besides nanofibers, films of chitosan/PEO blends obtained by solution casting were the subject of research. For such films, mechanical, structure and antibacterial studies were conducted [28]. DSC, nano-indentation and water uptake of the blend films were the subject of another article [29]. Miscibility, thermal analysis, biocompatibility were analyzed by other groups of researchers [30–34]. Also, hydrogel made of modified chitosan and PEO was prepared and characterized successfully [35].

The aim of this work was to study the surface and thermal properties of chitosan/PEO blends and mutual interactions between the blend components. Especially research on hydrophilicity and morphology of these blend surfaces enrich this work because such analyses have not been conducted. The next step was to study the photostability of these blends, which is the subject of another article.

Experimental

Chitosan was purchased from Aldrich. Molecular weight and degree of deacetylation were evaluated in our laboratory. Molecular weight was determined by viscometric measurements using Ubbelohde viscometer. The measurements were performed in 0.1 M CH_3COOH /0.2 M NaCl solution at 25°C. On the basis of these measurements, the limiting viscosity number, $[\eta]$, was obtained from the Huggins equation. Then, the viscosity-average molecular weight, \overline{M}_v , was calculated from the Mark-Houwink-Sakurada equation, $[\eta] = K\overline{M}_v^a$, where $K = 1.81 \times 10^{-3} \text{ cm}^3/\text{g}$ and $a = 0.93$ [36]. The viscosity-average molecular weight of chitosan was 411,000. To determine deacetylation degree, DD, of chitosan, the first derivative UV-spectrophotometry method was applied and DD was $82\% \pm 1.7\%$ [37].

Poly(ethylene oxide), $\overline{M}_w = 97,900$, was bought from Aldrich. This polymer was purified prior to use, i.e. it was dissolved in distilled water and then centrifuged to remove insoluble part. Transparent solution was cast on Petri glasses and after drying it was the material taken for the preparation of PEO solution.

2% (m/v) basic solutions of PEO and chitosan were prepared by dissolving PEO in distilled water and chitosan in 2% aqueous solution of acetic acid. Then, these solutions were mixed to

obtain 2% (m/v) solutions of polymeric blends with different component weight ratios. The solutions were transparent.

Next, the solutions were cast onto the levelled glasses in order to obtain thin polymeric films, which were first dried at ambient conditions and then carefully in an oven at 30°C. The films of the blends were opaque owing to the presence of PEO crystalline phase. The film thickness was about 30 μm to 70 μm .

ATR-FTIR spectra of chitosan/PEO films were collected using FTIR Genesis II (Mattson, USA) spectrophotometer equipped with ATR (Pike Technologies, Inc.) containing ZnSe crystal.

Contact angle measurements, surface free energies and polar and dispersion components were gained using a DSA G10 goniometer (Krüss GmbH, Germany). A drop of glycerol or diiodomethane was placed onto a sample surface with microsyringe and the value of contact angle was calculated by the computer on the basis of the obtained image of the liquid drop. The value of contact angle was average of ca. 8 measurements and the deviation from the average was within ± 2 deg. All measurements were carried out at room temperature.

AFM images were obtained with MultiMode NanoScope IIIa (Veeco Metrology Inc., USA) with silicon probe (Veeco) in a tapping mode in air at room temperature. The most typical images were chosen for presentation; additionally roughness parameters, R_a - an arithmetic mean, and R_q - a root mean square, were calculated for scan area $5\mu\text{m} \times 5\mu\text{m}$.

Differential scanning calorimetry (DSC) measurements were performed with a Netzsch Phoenix DSC 204 F1 (Germany). Samples of 5 mg were placed in aluminum crucibles with lids and sealed. A small hole was done in a lid to allow the moisture to evaporate. An empty crucible was used as a reference. All measurements were performed under nitrogen atmosphere with gas flow 40 ml/min. The following program was applied: cooling to 0°C and then heating to 100°C with heating rate 10°C/min, maintenance at 100°C for 5 min, cooling to 0°C with cooling rate 10°C/min. The DSC data were obtained from the first run. The melting temperature, T_m , was determined as the temperature at maximum of the endothermic peak, the melting enthalpy of PEO in the blends, ΔH_m , was determined from the area under the endothermic peak. The degree of crystallinity of PEO in the blend, X_c^m , was calculated according to the equation:

$$X_c^m = \Delta H_m / (f_w \bullet \Delta H_m^0),$$

where ΔH_m^0 is the melting enthalpy of 100% crystalline PEO, f_w is the weight fraction of PEO in the blend. ΔH_m^0 taken for calculation was 203 J/g [38].

X-ray diffraction (XRD) measurements were conducted on Philips X'Pert PRO diffractometer using $\text{CuK}\alpha$ radiation with the wavelength $\lambda = 1.54056\text{\AA}$. Cu-filtered radiation scanned the chitosan film in the 5–40° diffraction angle range.

Results and discussion

ATR-FTIR spectroscopy was applied to study the surface composition of the blends. This technique provides information from the film layer of several microns. Figure 1 shows ATR-FTIR spectra of chitosan, PEO and chitosan/PEO blends. ATR-FTIR spectrum of chitosan indicates a broad band in the range of 3000–3600 cm^{-1} attributed to stretching vibrations of hydrogen bonded O-H and N-H groups and also O-H/N-H interacting with oxygen from C=O group. The characteristic peaks at 1638 cm^{-1} and 1550 cm^{-1} can be assigned to the vibrations of C=O stretching (amide I) and N-H deformation (amide II) overlapping with NH_2 , respectively. In the region of 900–1200 cm^{-1} , three maxima at 1151 cm^{-1} , 1062 cm^{-1} ,

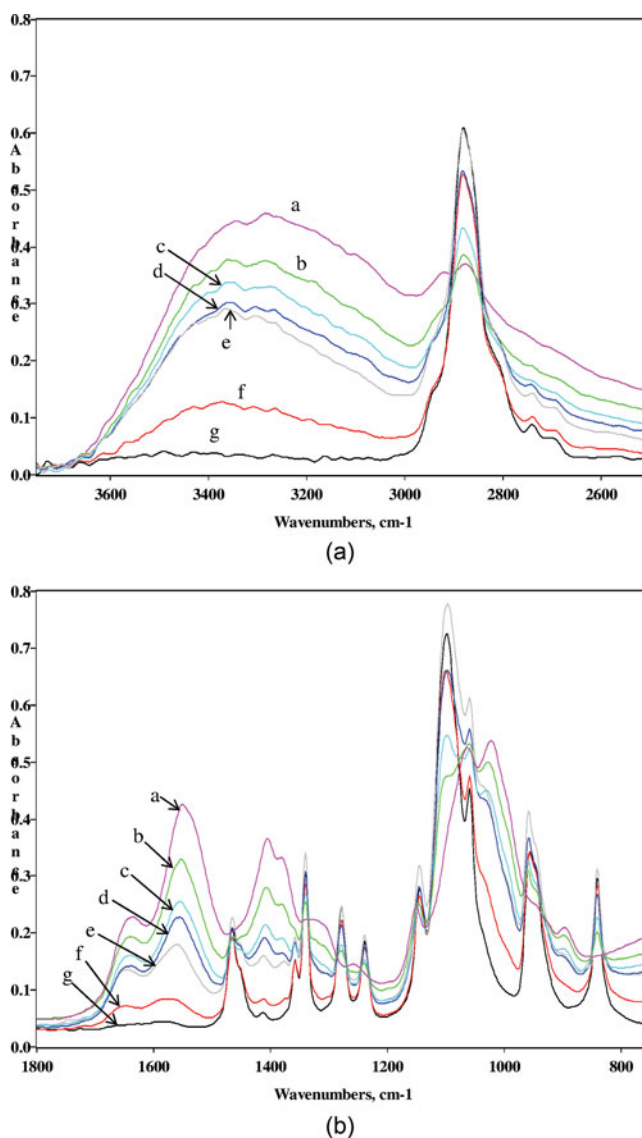
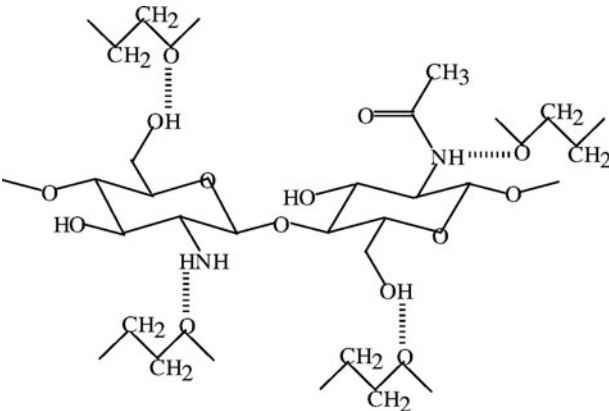


Figure 1. ATR-FTIR spectra of chitosan/PEO blend films with ratio: (a) 100/0, (b) 80/20 (c) 60/40, (d) 50/50, (e) 40/60 (f), 20/80, (g) 0/100.

1022 cm^{-1} are observed and they can be assigned to C–O–C vibrations of glucose rings and glycosidic linkages [21, 24, 28, 30–32].

For PEO, characteristic band with maxima at 1144 cm^{-1} , 1098 cm^{-1} and 1059 cm^{-1} can be assigned to vibrations of C–O–C, other absorption bands of this polymer are attributed to CH_2 vibrations. The ATR-FTIR spectrum of PEO exhibits bands characteristic of crystalline structure of this polymer: the presence of a doublet at 1357 cm^{-1} and 1340 cm^{-1} , a weak band at 1413 cm^{-1} and a triplet band at 1144 cm^{-1} , 1098 cm^{-1} , 1059 cm^{-1} [18, 30–32].

In the spectra of chitosan/PEO blends, one can distinguish absorption bands, characteristic of the pure polymers, with the intensity approximately proportional to the blend composition, which suggests that the bulk composition corresponds to the surface composition. Crystalline structure of PEO is recognizable in the samples with 40–100% of this polymer. In the studied



Scheme 1. Hydrogen bonds between chitosan and PEO.

blends, possible interactions between components could exist in the form of hydrogen bonds whose presence can be confirmed by the occurrence of shifts and broadening of suitable bands in infrared spectra. Hydrogen bonds are formed between proton-donor groups, for instance OH/NH₂ and NH of chitosan, and proton-acceptor groups, for instance C=O of chitosan and C–O–C of PEO (scheme 1).

Furthermore, proton-donor groups are also proton-acceptor groups, which leads to formations of hydrogen bonds within chitosan molecules [30–34]. Thus, the changes in the absorption bands of the groups which are capable of forming hydrogen bonds have been analyzed. Table 1 contains the values of absorption band maxima and their assignment to the appropriate bond vibrations, while Figure 1 shows the infrared spectra of the blends. One can observe the substantial shifts of the band maxima in the region of 3000–36000 cm^{−1} (~30 cm^{−1}), amide I (~10 cm^{−1}) and amide II (~30 cm^{−1}), also subtle shifts of ether band,

Table 1. Vibrational modes and absorption band maxima (cm^{−1}) for chitosan, PEO and the blends.

Vibrational modes	Wavenumbers (cm ^{−1})						
	Chitosan/PEO (wt.%)						
	100/0	80/20	60/40	50/50	40/60	20/80	0/100
OH, NH stretching	3342	3349	3357	3352	3365	3375	
	3283	3284	3285	3303	3302	3308	
CH stretching	2876	2879	2881	2881	2881	2881	2880
	2920						
C=O stretching (amide I)	1638	1640	1643	1643	1645	1648	
NH bending (amide II)	1550	1551	1553	1558	1560	1576	
CH ₂ scissoring	1404	1406	1408	1410	1412	1413	1413
CH ₂ scissoring		1465	1465	1465	1465	1465	1465
CH ₃ bending in amide group	1378	1378	1379	1379	1379		
CH wagging	1320	1340	1340	1340	1340	1340	1340
			1357	1357	1357	1357	1357
CH ₂ twisting	1257	1278	1278	1278	1278	1278	1278
		1239	1239	1239	1239	1238	1238
COC stretching	1151	1146	1146	1145	1145	1144	1144
		1099	1099	1097	1097	1099	1098
	1062	1059	1059	1059	1059	1059	1059
	1022	1025	1026	1029	1031	1034	
CH ₂ rocking		960	958	958	958	956	956
		840	840	840	840	840	840
CH ₂ rocking	896	896	896	896	896		

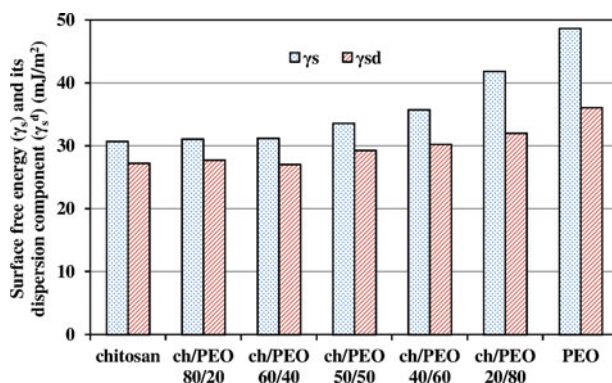


Figure 2. Surface free energy and dispersion component as a function of a sample composition.

however, the band maxima move towards higher wavenumbers. Band shifts towards lower wavenumbers indicate hydrogen bonding, which was not visible here. Moreover, ether band broadens towards lower wavenumbers when chitosan content in the blend increases and the greatest broadening of this band was noticed for the blend with 80% of chitosan. Such alterations in infrared spectra of the blends may suggest weak interactions between chitosan and PEO molecules, probably mainly at the interphase. Only in the case of the blend with 80% of chitosan, stronger interactions between the studied polymers occurred. In earlier works [31, 32], it was found that this blend, chitosan/PEO (80/20), was characterized by the strongest interactions between blend constituents owing to the formation of hydrogen bonds between hydroxyl/amino groups of chitosan and ether groups of PEO.

On the other hand, the presence of PEO may disturb intra and/or intermolecular hydrogen bonding between chitosan molecules resulting in band shifts towards higher wavenumbers. It is also possible that water molecules might be involved in the interactions. The OH, NH₂ and amide bands are influenced by the presence of moisture as the chitosan binds water using the mentioned groups [39, 40].

Generally, the results suggest weak interactions between the blend components. No changes in infrared spectra of chitosan/PEO films were found by Zivanovic et al. [28]. However, miscibility between chitosan and PEO due to hydrogen bonding was found by Rakkapao et al. [31], Wrzyszczyński et al. [33] and Khoo et al. [34]. Bostan's et al. studies demonstrated miscibility between chitosan and PEO but only in the blends with dominant chitosan content [30], which was also shown by Rakkapao et al. who applied molecular dynamic simulation to investigate the miscibility between chitosan and PEO [32].

Hydrophilicity of the sample surfaces was determined by contact angle measurements and surface free energy calculations. The results are presented in Figures 2 and 3. As can be seen, the values of polar components for all samples are much lower than the values of dispersion components, which means that the studied polymer surfaces are predominantly hydrophobic. The values of surface free energies and polar components are lower for chitosan compared to these values for PEO, which means that PEO has much more polar surface than chitosan. Hydrophobicity of chitosan can be explained by the fact that the polar groups are hidden beneath the surface and they are bound via hydrogen bonds. Relatively high hydrophilicity of PEO can result from the capability of ether oxygen of binding hydrogen from water or glycerol in this case [41]. Moreover, dispersion component of surface free energy for PEO (36.07 mJ/m²) is higher than that for chitosan (27.23 mJ/m²). It seems that the measuring

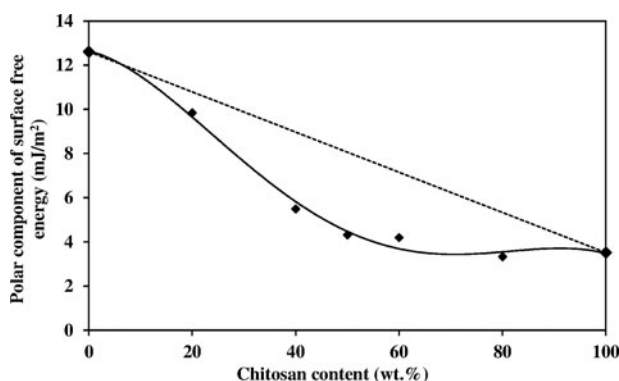


Figure 3. Polar component of surface free energy versus chitosan content in the blends. The dotted line shows theoretical values acquired on the basis of the additivity rule.

liquids interact with PEO by polar and dispersion forces stronger compared to chitosan [42]. The high value of surface free energy of PEO is caused by high value of polar and dispersion component.

In the case of the blends, the values of surface free energies and components are higher than that for chitosan and lower than that for PEO. Moreover, values of polar components are lower than it would be expected from the additivity rule, which means that the blend surfaces are more hydrophobic (Fig. 3). Probably more chitosan might appear on the blend surfaces as there is a tendency for lower surface free energy component to enrich the blend surfaces [43, 44]. Also in the case of the blends composed of amorphous and crystalline constituents, the amorphous one tends to locate at the surface region [45].

Surface enrichment in chitosan and levan was observed for the blends containing below 30% of PEO, whereas higher PEO content resulted in surface enrichment in PEO [30]. Zivanovic et al. [28] found that chitosan was dominant on the surfaces of the blends containing below 50% of PEO, while 50/50 blend revealed the surface composition corresponding to the bulk composition.

The AFM images of chitosan, PEO and the blends are shown in Figure 4. It is seen that surface morphology depends on sample composition. The chitosan surface is flat with fine-grained structure as this polymer is mainly amorphous, while PEO surface is heavily corrugated, which results from the presence of crystalline phase. The surface of chitosan/PEO (20/80) blend is similar to PEO surface owing to high amount of crystalline phase, whereas the surfaces of the other blends are different. One can observe hollows in the blend surfaces and these hollows become bigger when PEO content in the blends increases. However, the surface of the mixture with 60% of PEO is characterized by high flat hills and deep valleys and cleavages.

The observations are confirmed by roughness parameters, R_a and R_q (Fig. 5). Chitosan is characterized by the lowest values of the roughness parameters. The blend with 80% of this polymer is also characterized by relatively low values of these parameters compared to that for the other samples. Such behavior of this blend may be explained by the capability of PEO, which is present in a small amount in the chitosan matrix, to fill cavities in rigid chitosan chains [46] as PEO is much more flexible polymer ($T_g = -59^\circ\text{C}$) than chitosan ($T_g = 203^\circ\text{C}$) [31]. Moreover, interactions between hydroxyl and/or amine groups of

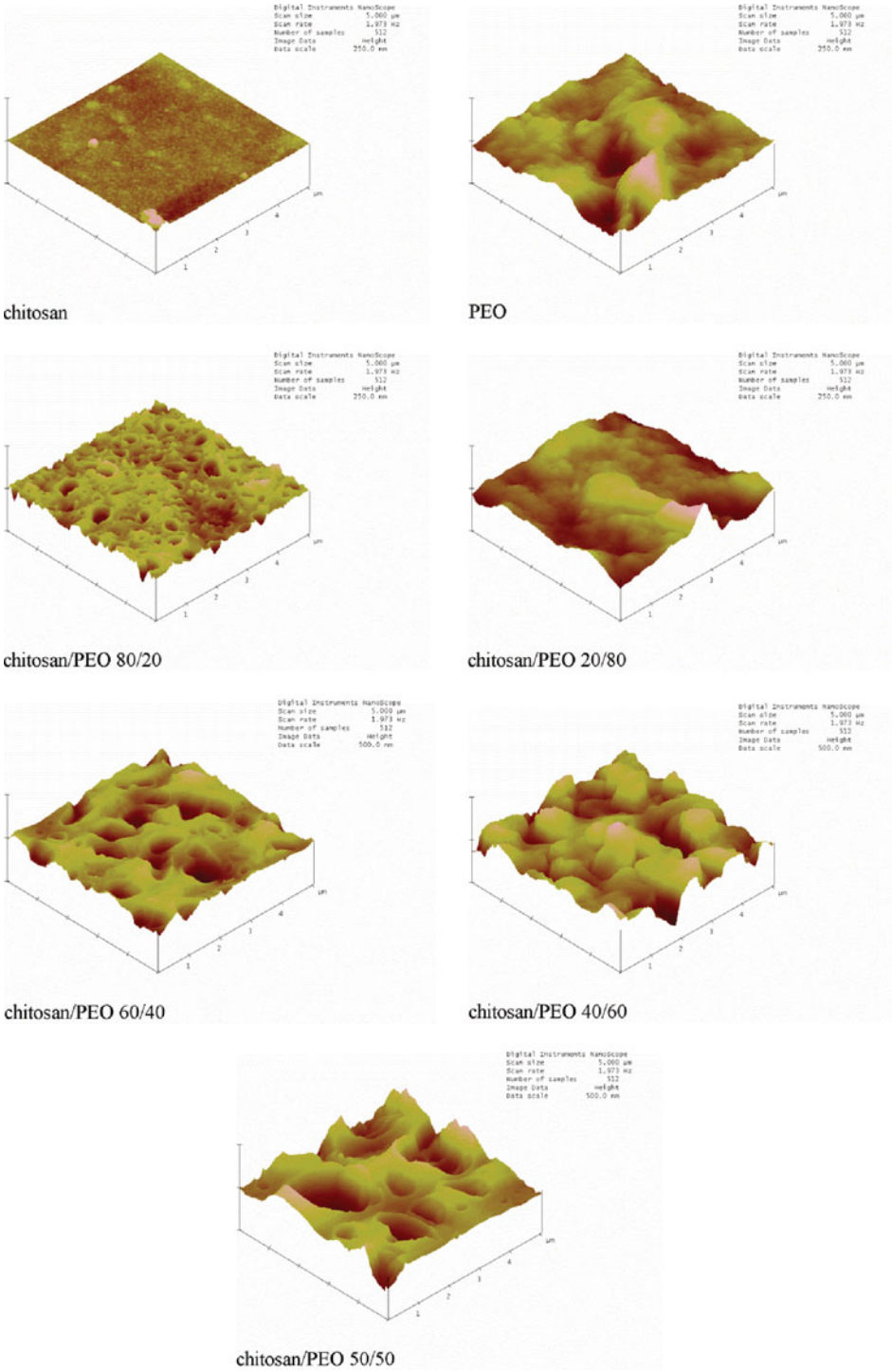


Figure 4. AFM height images of chitosan, PEO and chitosan/PEO blends. Scan area 5 μm × 5 μm. Z-scale: 250 nm for pure polymers and the blends with 80% of one component; z-scale: 500 nm for the remaining blends.

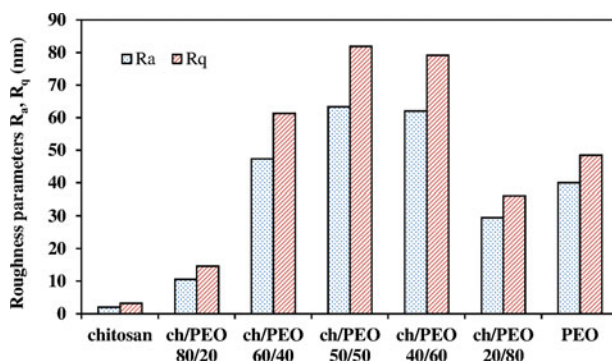


Figure 5. Roughness parameters, R_a , R_q , (nm) of the studied samples calculated for scan area $5 \mu\text{m} \times 5 \mu\text{m}$.

chitosan and ether groups of PEO can occur in this system, which was also confirmed by ATR-FTIR.

High R_a and R_q values for PEO are due to the crystalline state, typical of this polymer. In chitosan/PEO (20/80) blend, chitosan is in the minority and may be distributed in amorphous phase of PEO resulting in lower values of R_a and R_q than that for PEO. This blend may exhibit a partial miscibility.

The most pronounced growth in the roughness parameters was observed for the blends with 40–60% of PEO, which might be a result of the component immiscibility rather than the presence of crystalline phase of PEO as the roughness parameters are much higher for these blends compared to that for pure PEO. The immiscibility can be caused by repulsion forces between components resulting in substantial growth in the surface roughness.

DSC measurements enable us to record the melting temperature (T_m) and the melting enthalpy (ΔH_m) of a crystalline component in the blend. In the studied systems, PEO was semi-crystalline polymer thus its melting temperature and melting enthalpy was investigated in the 0–100°C range. To check whether the chitosan film possesses any crystalline phase, XRD pattern was obtained (Fig. 6). The broad peak of chitosan at $2\Theta = 21^\circ$ indicates amorphous nature of this polymer [47].

Figure 7 shows the melting endotherm of PEO in chitosan/PEO blends. It is seen that the maxima of endotherm shift towards lower temperatures and the areas under the curves clearly decline with increasing content of chitosan in the blends. In this temperature range, no melting behavior was observed for chitosan film. The data obtained from DSC measurements are presented in Figures 8 and 9. One can notice a slight decrease in T_m of PEO (6°C) in the blends (Fig. 8) and considerable drop in ΔH_m with increasing chitosan content (Fig. 9), which may be assigned to the dilution effect, except for the blend with 20% of PEO. Lowering T_m only

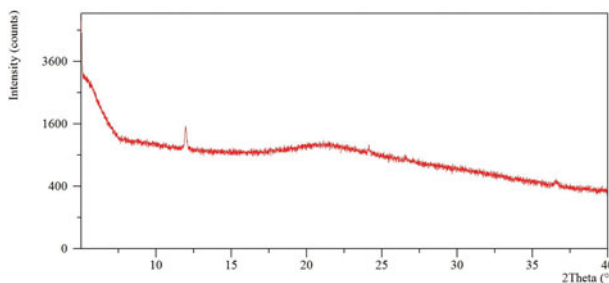


Figure 6. XRD pattern of chitosan film.

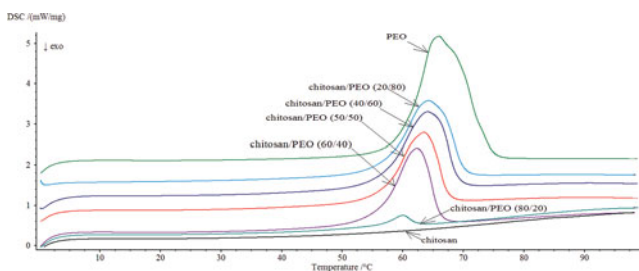


Figure 7. DSC curves of PEO, chitosan and chitosan/PEO blends.

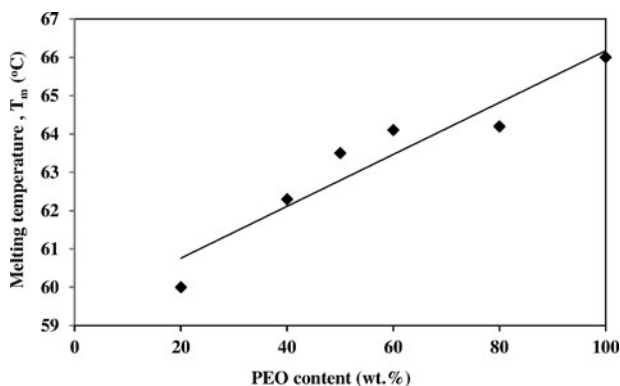


Figure 8. Melting temperature, T_m (°C), of PEO versus PEO content in the blends.

by 6°C over the 20–100% of PEO range composition may suggest weak interactions between polymers in the blends. Similar observations were made by other researchers, who also indicated that larger decrease in melting temperature was a result of stronger interactions between polymers in the blends [48–50]. However, the decrease in T_m and its relation to interactions in blends is not obvious because the reduction in T_m by about 3°–7°C was related to stronger interactions between blend components such as hydrogen bonds [31, 33, 46].

The degree of crystallinity (X_c^m) of PEO depends clearly on the blend composition (Fig. 9). Generally, X_c^m is high for the blends containing 40–80% of PEO, but slightly lower for the blend containing 80% of PEO and slightly higher for the blend with 40% of PEO, which suggests that in these blends between PEO and PEO molecules occur stronger interactions than between PEO and chitosan. The crystallization process of PEO was rather maintained in these

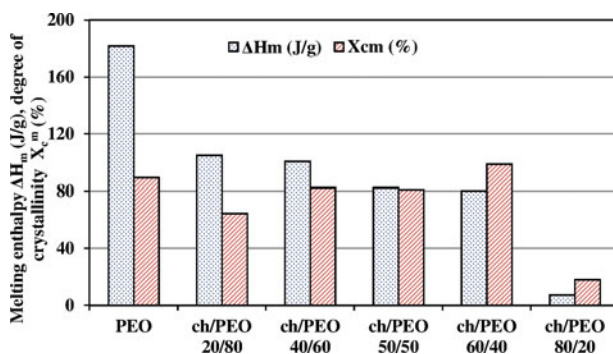


Figure 9. Melting enthalpy, ΔH_m (J/g), and the degree of crystallinity, X_c^m (%), as a function of a sample composition.

blends in the presence of chitosan, although some interactions between components at the interphase may occur in the blend with 80% of PEO, for which X_c^m was decreased by 30%.

However, a huge reduction in X_c^m , by about 80%, was observed for the blend with 20% of PEO, which suggests that chitosan affects interaction between PEO molecules and impedes formation of crystalline phase in this blend, probably owing to hydrogen bonding between hydroxyl and/or amine groups of chitosan and oxygen atom of PEO. Also flexible PEO molecules can fill cavities in a rigid chitosan structure.

DSC results suggested immiscibility or partial miscibility of chitosan and PEO molecules. Only the mixture composed of 20% of PEO and 80% of chitosan was found to be miscible. These findings are consistent with the result acquired by other methods.

Conclusions

On the basis of the conducted experiments, conclusions concerning interactions, miscibility, crystallinity, surface composition and morphology of chitosan/PEO blend films can be drawn.

Slight shifts or shifts towards higher wavenumbers of absorption bands in the infrared spectra of the studied blends, a considerable growth in roughness parameters, a small drop in melting temperatures and maintained high values of the degree of crystallinity could indicate weak interactions between chitosan and PEO in the blends leading to the immiscibility of the blend components. Only for chitosan/PEO (80/20) blend, the studies have revealed the presence of interactions owing to hydrogen bonding between hydroxyl and amine groups of chitosan and ether groups of PEO.

Hydrophilicity of the blend surfaces was lower than it would be expected from the additivity rule, which indicated the enrichment of the blend surfaces in chitosan, component of lower surface free energy.

Morphology of the blends was affected by the crystallinity of PEO and was dependent on the sample composition.

References

- [1] El-Hefian, E. A., Nasef, M. M., & Yahaya, A. B. (2014). *J. Chem. Soc. Pak.*, 36, 11.
- [2] Aramwit, P., Ekasit, S., & Yamdech, R. (2015). *Biomed. Microdevices*, 17, 84.
- [3] Shigehiro, H., Haruyoshi, S., Yasutoshi, A., & Isao, N. (1988). *Polym. Mater. Sci. Eng., Proc. ACS Div. Polym. Mater. Sci. Eng.*, 58, 897.
- [4] Felt, O., Furrer, P., Mayer, J.M., Plazonnet, B., Buri, P., & Gurny, R. (1999). *Int. J. Pharm.*, 180, 185.
- [5] Muzzarelli, R. A. A. (1997). *Cell. Mol. Life Sci.*, 53, 131.
- [6] Zivanovic, S., Chi, S., & Draughon, A. E. (2005). *J. Food Sci.*, 70, 45.
- [7] Remya, S., Mohan, C. O., Bindu, J., Sivaraman, G. K., Vankateshwarlu, G., & Ravishankar, C. N. (2016). *J. Food Sci. Technol.*, 53, 685.
- [8] Wu, W., Shen, J., Banerjee, P., & Zhou, S. (2010). *Biomaterials*, 31, 8371.
- [9] Ong, S.-J., Wu, J., Moomchala, S. M., Tang, M.-H., & Lu, J. (2008). *Biomaterials*, 29, 4323.
- [10] Patrulea, V., Ostafe, V., Borchard, G., & Jordan, O. (2015). *Eur. J. Pharm. Biopharm.*, 97, 417.
- [11] Muzzarelli, R. A. A. (1996). *Carbohydr. Polym.*, 29, 309.
- [12] Scalia, S., Trotta, V., Iannuccelli, V., & Bianchi, A. (2015). *Colloids Surf., B*, 135, 42.
- [13] Rhazi, M., Desbrières, J., Tolaimate, A., Rinaudo, M., Vottero, P., Alagui, A., & El Meray, M. (2002). *Eur. Polym. J.*, 38, 1523.
- [14] Crini, G., Badot, P.-M. (2008). *Prog. Polym. Sci.*, 33, 399.
- [15] Zeng, D., Luo, X., & Tu, R. (2012). *Int. J. Carbohydr. Chem.*, ID, 104565, 1.
- [16] Grillo, R., Rosa, A. H., & Fraceto, L. F. (2014). *Int. J. Environ. Sci. Technol.*, 11, 1691.
- [17] MacCallum, J. R., Vincent, C. A. (1997). *Polymer Electrolyte Reviews-1*, Elsevier Applied Science Publishers LTD: London, UK.

- [18] Bailey F. E. Jr, & Koleske, J. V. (1976). *Poly(ethylene oxide)*, Academic Press: New York, USA.
- [19] Israelachvili, J. (1997). *Proc. Natl. Acad. Sci.*, 94, 8378.
- [20] Desai, K., Kit, K., Li, J., & Zivanovic, S. (2008). *Biomacromolecules*, 9, 1000.
- [21] Dorraki, N., Safa, N. N., Jahanfar, M., Ghomi, H., & Ranaei-Siadat, S.-O. (2015). *Appl. Surf. Sci.*, 349, 940.
- [22] Erdem, R., & Akalin, M. (2015). *J. Ind. Text.*, 44, 553.
- [23] Dilamian, M., Montazer, M., & Masoumi, J. (2013). *Carbohydr. Polym.*, 94, 364.
- [24] Kriegel, C., Kit, K. M., McClements, D. J., & Weiss, J. (2009). *Polymer*, 50, 189.
- [25] Cassani, D. A. D., Altomare, L., De Nardo, L., & Variola, F. (2015). *J. Mater. Chem. B*, 3, 2641.
- [26] Bizarria, M. T. M., d'Ávila, M. A., & Mei, L. H. I. (2014). *Braz. J. Chem. Eng.*, 31, 57.
- [27] Barchuk, M., Čapková, P., Kolská, Z., Matoušek, J., Poustka, D., Šplíchalová, L., Benada, O., & Munzarová, M. (2016). *J. Polym. Res.*, 23, 20.
- [28] Zivanovic, S., Li, J., Davidson, P. M., & Kit, K. (2007). *Biomacromolecules*, 8, 1505.
- [29] Djokić, J. D., Kojović, A., Stojanović, D., Marinković, A., Vuković, G., Aleksić, R., & Uskoković, P. S. (2012). *J. Serb. Chem. Soc.*, 77, 1723.
- [30] Bostan, M. S., Mutlu, E. C., Kazak, H., Keskin, S. S., Oner, E. T., & Eroglu, M. S. (2014). *Carbohydr. Polym.*, 102, 993.
- [31] Rakkapao, N., Vao-soongnern, V., Masubuchi, Y., & Watanebe, H. (2001). *Polymer*, 52, 2618.
- [32] Rakkapao, N., & Vao-soongnern, V. (2014). *J. Polym. Res.*, 21, 606.
- [33] Wrzyszczyński, A., Qu, X., Szosland, L., Adamczak, E., Lindén, L. Å, & Rabek, J. F. (1995). *Polym. Bull.*, 34, 493.
- [34] Khoo, C. G. L., Frantzich, S., Rosinski, A., Sjöström, M., & Hoogstraate, J. (2003). *Eur. J. Pharm. Biopharm.*, 55, 47.
- [35] Kim, D., Kim, S., Jo, S., Woo, J., & Noh, I. (2011). *Macromol. Res.*, 19, 396.
- [36] Robert, G.A.F., & Domszy, J.G. (1982). *Int.J. Biol. Macromol.*, 4, 374.
- [37] Trzciński, S., Szulc, D., & Staszewska, D. U. (2000). *Progress on Chemistry and Application of Chitin and Its Derivatives*, VI, Łódź, Poland.
- [38] Huang, X. D., & Goh, S. H. (2002). *Polymer*, 43, 1417.
- [39] Neto, C. G. T., Giacometti, J. A., Job, A. E., Ferreira, F. C., Fonseca, J. L. C., & Pereira, M. R. (2005). *Carbohydr. Polym.*, 62, 97.
- [40] Rueda, D. R., Secall, T., & Bayer, R. K. (1999). *Carbohydr. Polym.*, 40, 49.
- [41] Morra, M. (2001). *Water in Biomaterials Surface Science*, John Wiley & Sons Ltd: Chichester, UK.
- [42] Chibowski, E., & Terpilowski, K. (2008). *J. Colloid Interface Sci.*, 319, 505.
- [43] Boyd, R. D., & Badyal, J. P. S. (1997). *Macromolecules*, 30, 5437.
- [44] Çaykara, T., Demirci, S., Eroglu, M. S., & Güven, O. (2005). *Polymer*, 46, 10750.
- [45] Affrossman, S., Kiff, T., O'Neill, S., Pethrick, R. A., & Richards, R. W. (1999). *Macromolecules*, 32, 2721.
- [46] Sashina, E. S., Vnuchkin, A. V., & Novoselov, N. P. (2006). *Russ. J. Appl. Chem.*, 79, 1643.
- [47] Celebi, H., & Kutur, A. (2015). *Carbohydr. Polym.*, 1333, 284.
- [48] Belfiore, L. A., Lee, C. K. S., & Tang, J. (2003). *Polymer*, 44, 3333.
- [49] Rocco, A. M., Moreira, D. P., & Pereira, R. P. (2003). *Eur. Polym. J.*, 39, 1925.
- [50] Silva, E. F., Pereira, R. P., & Rocco, A. M. (2009). *Eur. Polym. J.*, 45, 3127.